

A Nonhomogeneous Kinetic Model of Liquid Crystal Polymers and Its Thermodynamic Closure Approximation

Haijun Yu^{1,*}, Guanghua Ji² and Pingwen Zhang¹

¹ LMAM, School of Mathematical Sciences and CCSE, Peking University, Beijing 100871, China.

² Laboratory of Mathematics and Complex Systems, Ministry of Education and School of Mathematical Sciences, Beijing Normal University, Beijing 100875, China.

Received 12 February 2009; Accepted (in revised version) 12 June 2009

Available online 24 August 2009

Abstract. A general nonhomogeneous extension of the Doi's kinetic theory with translational diffusion and nonlocal potential is proposed to describe the microstructures and defect dynamics of Liquid Crystal Polymer (LCP) solutions. The long-range elasticity of polymer molecules is depicted by a kernel type potential, from which one can derive the well-known Marrucci-Greco potential with weak spatial distortion assumption. Applying quasi-equilibrium closure approximation, we get a second-order moment model for isotropic long-range elasticity, and this reduced moment model maintains the energy dissipation. Implemented by the invariant-based fitting method, the moment model is a decent tool for numerical simulations of defect dynamics and texture evolution in LCP solutions. The numerical results of in-plane rotational case show that the reduced second-order moment model qualitatively predicts complicated nonhomogeneous director dynamics under moderate nematic potential strength, and the translational diffusion plays an important role in defect dynamics.

PACS: 61.30.Cz, 61.30.Dk, 61.30.Vx

Key words: LCP, kinetic theory, energy dissipation, closure approximation, defect dynamics.

1 Introduction

The kinetic theory of LCPs, started from Hess [16] and developed by Doi etc. [4, 5], has been a popular topic for three decades. The Doi-Hess theory predicts plenty of director dynamics in homogeneous nematic LCP solutions, such as tumbling, wagging, flow-aligning and log-rolling [9, 10, 26] etc. The interaction between the inner bulk tumbling

*Corresponding author. *Email addresses:* yuhaijun@gmail.com (H. Yu), ghji@bnu.edu.cn (G. Ji), pzhang@pku.edu.cn (P. Zhang)

region and boundary anchoring layer introduces defects and complex microstructures in nonhomogeneous LCP solutions. Meanwhile, these defects and microstructures strongly influence the rheology of the solutions. Marrucci and Greco [27] first analyzed the long-range elasticity of LCPs by introducing a nonlocal intermolecular potential based on the Maier-Saupe potential. Some nonhomogeneous extensions of Doi's theory, differing in the intermolecular potential, have been presented. Feng, Sgarlari and Leal [8] adopted a one-constant Marrucci-Greco potential; Wang, E, Liu and Zhang [31] adopted an integral form potential; and Wang [30] extended the Marrucci-Greco potential to account for macromolecules with different shapes. Although these nonhomogeneous kinetic theories have appeared for several years, 2D and 3D numerical studies based on them are sparse, because of huge computational cost involved. However, reduced equations about the moments of configuration distribution function (CDF) can be obtained from the exact kinetic models. The problem is that the equations of lower-order moments of CDF obtained from kinetic theory are coupled with higher-order moments. To close these equations, one must express higher-order moments in terms of lower-order moments, which is the so-called closure approximation.

Closure approximations for complex materials have been under investigation for many years. Various closure approximations have been proposed, such as the Doi's quadratic closure [5], the HL closures [17], orthotropic closure [3] and the Bingham closure [1]. Feng et al. [7] provided detailed numerical comparisons among five commonly used closures and found that the Bingham closure gives better results than others, although it deviates from the solutions of the exact kinetic theory when both the shear rate and nematic potential strength are very big. In fact, the Bingham closure is a particular case of quasi-equilibrium closure approximation (QEA). The systemic depiction of QEA is given by Gorban and the coworkers [11–14]. Ilg, Karlin and Öttinger [21] applied QEA to flexible polymers in homogeneous systems, while Ilg, Karlin, Kröger and Öttinger [20] analyzed rod-like polymers. They proved that QEA maintains the energy dissipation for homogeneous systems when flow is absent.

In our opinion, there are four criteria to evaluate closure approximations. First of all, the reconstructed CDF should be positive; secondly, a good closure approximation should maintain thermodynamic properties, such as mass conservation and energy dissipation; thirdly, it should achieve good accuracy; the last but not the least, a low computational cost implementation can be established for nonhomogeneous simulations. Energy dissipation is a basic requirement in the modeling of dissipation systems. However, it was not considered in the closure approximations of LCP kinetic theory until the work of Ilg et al. [21] was published. From the thermodynamic point of view, QEA is the proper closure approximation, but the numerical integration scheme for QEA proposed by Ilg et al. [19] is too expensive for nonhomogeneous simulation.

We introduce a relatively simple but general nonhomogeneous kinetic model for LCPs, and develop an efficient reduced moment model by QEA, which maintains energy dissipation. The invariant-based fitting method [2,22,29] is adopted in the simulations to reduce the computational costs.

The paper is organized as follows. First, we present a nonhomogeneous extension of the Doi kinetic theory. In Section 3, we deduce the reduced second-order moment model of LCP with isotropic long-range elasticity, and show how the Bingham closure approximation maintains energy dissipation. The numerical simulation of the in-plane rotational problem in nonhomogeneous flow will be given in Section 4. We give our conclusion at the end of the paper.

2 A nonhomogeneous extension of the Doi kinetic theory

We study LCP solutions containing N liquid crystalline polymer molecules in space Ω with volume V . Then the average number density is $\bar{v} = N/V$. The configuration distribution function $f(\mathbf{x}, \mathbf{m}, t)$ denotes the number density of LCP molecules located at spatial position \mathbf{x} with orientation \mathbf{m} at time t . The conservation of the number of LCP molecules is given by

$$\int_{\Omega} \int_{|\mathbf{m}|=1} f(\mathbf{x}, \mathbf{m}, t) d\mathbf{m} d\mathbf{x} = N. \tag{2.1}$$

For convenience, we denote the ensemble average with respect to f by angle brackets

$$\langle (\cdot) \rangle = \int_{|\mathbf{m}|=1} (\cdot) f(\mathbf{x}, \mathbf{m}, t) d\mathbf{m}.$$

The moments of the CDF are given by $M_i = \langle \mathbf{m}^i \rangle$, $i = 2, 4, 6, \dots$. Here \mathbf{m}^i stands for the tensor product of several values of \mathbf{m} . Particularly, we denote M_2, M_4, M_6 by M, Q, P and $\nu(\mathbf{x}, t) = \langle 1 \rangle$ is the number density of LCP molecules at the spatial position \mathbf{x} .

Following the procedure similar to Wang et al. [31], we deduce the hydrodynamic-kinetic coupled model in this section. The main difference is that we adopt a simpler mean-field potential. We believe this potential is good enough to some extent, as it can be reduced to the well-known Marrucci-Greco potential.

2.1 Smoluchowski equation

We assume that the excluded-volume potential for nonhomogeneous LCP solutions takes the form

$$U(\mathbf{x}, \mathbf{m}, t) = \int_{|\mathbf{m}'|=1} \int_{\Omega} G(\mathbf{x} - \mathbf{x}', \mathbf{m}, \mathbf{m}') f(\mathbf{x}', \mathbf{m}', t) d\mathbf{x}' d\mathbf{m}', \tag{2.2}$$

where $G(\mathbf{x} - \mathbf{x}', \mathbf{m}, \mathbf{m}')$ denotes the mean-field interaction between two molecules located at spatial position \mathbf{x} with orientation \mathbf{m} and at position \mathbf{x}' with orientation \mathbf{m}' . We will discuss the kernel G in detail at the end of this section.

The free energy of the system is given by

$$A[f] = \int_{\Omega} \int_{|\mathbf{m}|=1} \left(f \ln f - f + \frac{1}{2} f U \right) d\mathbf{m} d\mathbf{x}. \tag{2.3}$$

Then the chemical potential is

$$\mu = \frac{\delta A}{\delta f} = \ln f + U. \quad (2.4)$$

With free energy, the Smoluchowski equation of $f(\mathbf{x}, \mathbf{m}, t)$ for LCP solution under shear (see also [5, 31]) can be specified as

$$\begin{aligned} \frac{\partial f}{\partial t} + \nabla \cdot (\mathbf{u}f) = \nabla \cdot \left\{ [D_{\parallel} \mathbf{m}\mathbf{m} + D_{\perp} (I - \mathbf{m}\mathbf{m})] \cdot (f \nabla \mu) \right\} \\ + \mathcal{R} \cdot \left(D_r(\mathbf{m}) (f \mathcal{R} \mu) \right) - \mathcal{R} \cdot (\mathbf{m} \times \kappa \cdot \mathbf{m} f), \end{aligned} \quad (2.5)$$

where $\nabla = (\partial/\partial x, \partial/\partial y, \partial/\partial z)$, $\mathcal{R} = \mathbf{m} \times \partial/\partial \mathbf{m}$. D_{\parallel}, D_{\perp} are coefficients of translational diffusion parallel and perpendicular to the local molecular orientation, and $D_r(\mathbf{m})$ is orientational diffusion coefficient, which depends on the orientation of molecules in nematic phase:

$$D_r(\mathbf{m}) = D_{r0} \left[\frac{4}{\pi} \int_{|\mathbf{m}'|=1} |\mathbf{m} \times \mathbf{m}'| f(\mathbf{x}, \mathbf{m}', t) d\mathbf{m}' \right]^{-2}.$$

It is often pre-averaged and approximated by order tensor $S = \langle \mathbf{m}\mathbf{m} - \frac{1}{3} \rangle$ as

$$\bar{D}_r \approx D_{r0} \left(1 - \frac{3}{2} S : S \right)^{-2}. \quad (2.6)$$

Usually, the coefficient of spatial translational diffusion is much smaller than the coefficient of orientational diffusion, but it should not be omitted in nonhomogeneous simulations. The numerical simulations by Yu and Zhang [32] showed that the anisotropic translational diffusion ($D_{\parallel} \neq D_{\perp}$) plays an important role in defect dynamics. We will also discuss it in numerical results of the reduced model.

2.2 Hydrodynamic equation

The continuity equation of the system is

$$\frac{\partial \rho}{\partial t} + \nabla \cdot (\rho \mathbf{u}) = 0. \quad (2.7)$$

Here ρ is the total density of the solution, it may depend on the number density ν ,

$$\rho = \rho(\nu(x)). \quad (2.8)$$

The momentum equation reads

$$\rho \frac{d\mathbf{u}}{dt} = -\nabla p + \eta_s \Delta \mathbf{u} + \nabla \cdot \boldsymbol{\tau}^p + \mathbf{F}^e, \quad (2.9)$$

where $\frac{d}{dt} = \frac{\partial}{\partial t} + (\mathbf{u} \cdot \nabla)$ is the material derivative, η_s is the solvent viscosity, τ^p is the polymer stress, and \mathbf{F}^e is body force introduced by spatial variation of $f(\mathbf{x}, \mathbf{m}, t)$. The polymer stress is given by two parts, the viscous stress τ^s and the elastic stress τ^e :

$$\tau^p = \tau^s + \tau^e.$$

According to the Doi's theory,

$$\tau^s = \zeta_r D : \langle \mathbf{m m m m} \rangle,$$

where

$$D = \frac{1}{2}(\kappa + \kappa^T) = \frac{1}{2}(\nabla \mathbf{u} + (\nabla \mathbf{u})^T)$$

is the strain rate tensor, ζ_r is the coefficient of friction for solvent.

The elastic stress and body force can be derived through a generalized virtual work principle:

$$\tau^e = -\langle \mathbf{m m} \times \mathcal{R} \mu \rangle, \tag{2.10}$$

$$\mathbf{F}^e = - \int_{|\mathbf{m}|=1} \nabla U f(\mathbf{x}, \mathbf{m}, t) d\mathbf{m} = -\langle \nabla U \rangle, \tag{2.11}$$

see, e.g., [6] for more details.

Eqs. (2.5), (2.7)-(2.9) form a well-posed system. If $d\rho/dv \neq 0$, the solution is not a standard incompressible fluid. Although the density of solution has no relationship to pressure, the density is not constant because of the spatial translational diffusion of polymer molecules. One may regard Eqs. (2.7) and (2.9) as incompressible system and the divergence of velocity is given by

$$\nabla \cdot \mathbf{u} = -\frac{1}{\rho} \frac{d\rho}{dt} = -\frac{1}{\rho} \frac{d\rho}{dv} \frac{dv}{dt}. \tag{2.12}$$

If $d\rho/dv = 0$, the solution becomes standard incompressible fluid: ρ is a constant and the incompressible condition $\nabla \cdot \mathbf{u} = 0$ is satisfied. For simplicity, we only discuss the standard incompressible case in the rest of this paper.

Remark 2.1. The kinetic-Hydrodynamic coupled system has very good thermodynamic properties, such as mass conservation and energy dissipation. The detailed derivation of energy dissipation was presented in [31].

2.3 Intermolecular potential

There are many excluded-volume potentials, for example, the Onsager potential, the Maier-Saupe potential, the Marrucci-Greco potential [27] and some other nonlocal potentials with integral forms given by Wang et al. [31] and E et al. [6]. Here, we present a kernel type potential with a specific integral kernel

$$G(\mathbf{x} - \mathbf{x}', \mathbf{m}, \mathbf{m}') = U_0 \frac{g(\mathbf{x}' - \mathbf{x}, \mathbf{m}) + g(\mathbf{x}' - \mathbf{x}, \mathbf{m}')}{2} |\mathbf{m} \times \mathbf{m}'|^2, \tag{2.13}$$

where U_0 is nematic potential strength determined by the average number density of LCP, the size and the shape of LCP molecules; $|\mathbf{m} \times \mathbf{m}'|^2$ accounts for Maier-Saupe nematic interaction, $g(\mathbf{x}' - \mathbf{x}, \mathbf{m})$ accounts for long range interaction. We assume that the iso-surface of the long range interaction is spheroidal surface, i.e.,

$$g(\mathbf{y}, \mathbf{m}) = \frac{1}{\varepsilon_1 \varepsilon_2^2} g \left(\frac{(\mathbf{y} \cdot \mathbf{m})^2}{\varepsilon_1^2} + \frac{|\mathbf{y}|^2 - (\mathbf{y} \cdot \mathbf{m})^2}{\varepsilon_2^2} \right), \quad (2.14)$$

where ε_1 and ε_2 are the characteristic interaction distance parallel and perpendicular to \mathbf{m} , respectively; $g(r)$ is a normalized weight function. For simplicity, we take

$$g(r) = \begin{cases} C \exp\{\frac{1}{r^2-1}\}, & |r| \leq 1, \\ 0, & |r| > 1, \end{cases}$$

where C is the normalization constant.

In some special cases, the potential with the integral kernel (2.14) can be reduced to some well known potentials, such as Maier-Saupe potential, Marrucci-Greco potential etc.

1. For homogeneous systems, $f(\mathbf{x}', \mathbf{m}', t) = f(\mathbf{x}, \mathbf{m}', t)$. Then (2.2) becomes the Maier-Saupe potential

$$U_{MS}(\mathbf{x}, \mathbf{m}, t) = U_0 \int_{|\mathbf{m}'|=1} |\mathbf{m} \times \mathbf{m}'|^2 f(\mathbf{x}, \mathbf{m}', t) d\mathbf{m}'. \quad (2.15)$$

Alternatively, we can obtain it by taking the limits $\varepsilon_1 = \varepsilon_2 \rightarrow 0$ in Eq. (2.14).

2. If the variation of $f(\mathbf{x}, \mathbf{m}, t)$ along spatial direction \mathbf{x} is small, then $f(\mathbf{x}', \mathbf{m}', t)$ can be approximated by its second-order Taylor series with respect to \mathbf{x}' at \mathbf{x} ,

$$f(\mathbf{x}, \mathbf{m}', t) + \nabla f(\mathbf{x}, \mathbf{m}', t) \cdot (\mathbf{x}' - \mathbf{x}) + \frac{1}{2} \nabla^2 f(\mathbf{x}, \mathbf{m}', t) : (\mathbf{x}' - \mathbf{x})(\mathbf{x}' - \mathbf{x}).$$

Putting this series into (2.2) gives

$$\begin{aligned} U(\mathbf{x}, \mathbf{m}, t) &= U_{MS} + U_0 \int_{|\mathbf{m}'|=1} \int_{\Omega} \left\{ \frac{g(\mathbf{x}' - \mathbf{x}, \mathbf{m}) + g(\mathbf{x}' - \mathbf{x}, \mathbf{m}')}{4} |\mathbf{m} \times \mathbf{m}'|^2 \right. \\ &\quad \left. \times \nabla^2 f(\mathbf{x}, \mathbf{m}', t) : (\mathbf{x}' - \mathbf{x})(\mathbf{x}' - \mathbf{x}) \right\} d\mathbf{x}' d\mathbf{m} \\ &= U_{MS} + U_0 \int_{|\mathbf{m}'|=1} \left\{ |\mathbf{m} \times \mathbf{m}'|^2 \nabla^2 f(\mathbf{x}, \mathbf{m}', t) \right. \\ &\quad \left. : \int_{\Omega} \frac{g(\mathbf{x}' - \mathbf{x}, \mathbf{m}) + g(\mathbf{x}' - \mathbf{x}, \mathbf{m}')}{4} (\mathbf{x}' - \mathbf{x})(\mathbf{x}' - \mathbf{x}) d\mathbf{x}' \right\} d\mathbf{m}' \end{aligned}$$

$$\begin{aligned}
 &= U_{MS} + U_0 \int_{|\mathbf{m}'|=1} \left\{ (1 - \mathbf{m}\mathbf{m} : \mathbf{m}'\mathbf{m}') \nabla^2 f(\mathbf{x}, \mathbf{m}', t) \right. \\
 &\quad \left. : \left(\frac{1}{5} \varepsilon_2^2 I + \frac{1}{10} (\varepsilon_1^2 - \varepsilon_2^2) (\mathbf{m}\mathbf{m} + \mathbf{m}'\mathbf{m}') \right) \right\} d\mathbf{m}' \\
 &= U_0 \left[(1 + c_1 \Delta) (\nu I - M) : \mathbf{m}\mathbf{m} \right. \\
 &\quad \left. + \frac{c_2}{2} (\nabla^2 (\nu I - M) :: \mathbf{m}\mathbf{m}\mathbf{m}\mathbf{m} + \nabla^2 : (MI - Q) : \mathbf{m}\mathbf{m}) \right], \tag{2.16}
 \end{aligned}$$

where

$$c_1 = \frac{1}{5} \varepsilon_2^2, \quad c_2 = \frac{1}{5} (\varepsilon_1^2 - \varepsilon_2^2).$$

If we ignore the translational diffusion term in Eq. (2.5), then ν does not depend on \mathbf{x} , and Eq. (2.16) leads to the symmetric form of the Marrucci-Greco potential.

3. If the long-range elasticity is isotropic, i.e. $\varepsilon_1 = \varepsilon_2 = \varepsilon$, then

$$g(\mathbf{x}' - \mathbf{x}, \mathbf{m}) = \frac{1}{\varepsilon^3} g(|\mathbf{x}' - \mathbf{x}|^2 / \varepsilon^2) = g_\varepsilon(\mathbf{x}' - \mathbf{x}).$$

Consequently,

$$\begin{aligned}
 U(\mathbf{x}, \mathbf{m}, t) &= U_0 \int_{\Omega} \int_{|\mathbf{m}'|=1} g_\varepsilon(\mathbf{x}' - \mathbf{x}) |\mathbf{m} \times \mathbf{m}'|^2 f(\mathbf{x}', \mathbf{m}', t) d\mathbf{m}' d\mathbf{x}' \\
 &= U_0 g_\varepsilon * (\nu I - M) : \mathbf{m}\mathbf{m}. \tag{2.17}
 \end{aligned}$$

Using local expansion similar to case 2 above, we can get a slightly simplified form of the Marrucci-Greco potential, which was used by Klein et al. [24, 25]. Moreover, for the sake of simplicity, we will assume that the long-range elasticity is isotropic in the rest of our paper.

As shown above, the intermolecular potential with the integral kernel (2.13) leads to the Marrucci-Greco potential when the spatial variation of CDF is small. The constants c_1, c_2 in the Marrucci-Greco potential only depend on the characteristic interaction distance $\varepsilon_1, \varepsilon_2$, but do not depend on the special form of $g(r)$. Compared to the differential type potentials, the emergence of the body force (2.11) is also an advantage of integral type potentials.

Remark 2.2. For anisotropic long-range intermolecular potential, i.e. $\varepsilon_1 \neq \varepsilon_2$, the intermolecular potential

$$U(\mathbf{x}, \mathbf{m}) = U_0 \iint \frac{g(\mathbf{x} - \mathbf{x}', \mathbf{m}) + g(\mathbf{x} - \mathbf{x}', \mathbf{m}')}{2} |\mathbf{m} \times \mathbf{m}'|^2 f(\mathbf{x}', \mathbf{m}') d\mathbf{x}' d\mathbf{m}' \tag{2.18}$$

cannot be rewritten into the form

$$U(\mathbf{x}, \mathbf{m}) = \varphi(M) : \mathbf{m}\mathbf{m}. \tag{2.19}$$

Thus, we need to simplify Eq. (2.18) to some extent. Using the cumulant expansion, which was used by Ilg et al. [18], we can get an approximation of intermolecular potential,

$$U_1(\mathbf{x}, \mathbf{m}) = \frac{U_0}{\varepsilon_1 \varepsilon_2^2} \left[\int \frac{g\left(\frac{\mathbf{y}^2}{\varepsilon_2^2} + c\mathbf{y}^2 : M_{\mathbf{x}}\right) + g\left(\frac{\mathbf{y}^2}{\varepsilon_2^2} + c\mathbf{y}^2 : M_{\mathbf{x}'}\right)}{2} (v_{\mathbf{x}'I - M_{\mathbf{x}'}}) d\mathbf{x}' \right] : \mathbf{m}\mathbf{m}.$$

Here $c = 1/\varepsilon_1^2 - 1/\varepsilon_2^2$ and $\mathbf{y} = \mathbf{x} - \mathbf{x}'$.

The validity of this approximation needs to be verified by numerical simulations.

3 Second-order moment model

Solving Eq. (2.5) in two- and three-dimensional nonhomogeneous cases directly is very expensive. Fortunately, not all the CDF information is necessary for evaluating macroscopic physical properties. As the stress only involves the second-order and fourth-order moments of f , a straightforward idea is to derive moment equations from kinetic equation (2.5) to reduce the computational cost.

Multiplying Eq. (2.5) by $\mathbf{m}\mathbf{m}$ and then integrating both sides of the resulting equation with respect to \mathbf{m} on unit sphere, together with the isotropic long-range elasticity intermolecular potential (2.17) and pre-averaged approximation of $D_r(\mathbf{m})$ given in (2.6), we obtain the evolution equation for second moments M , which involve fourth-order moments Q and sixth-order moments P

$$\frac{dM}{dt} = \frac{dM_p}{dt} + \frac{dM_r}{dt} + \frac{dM_u}{dt}, \quad (3.1a)$$

where

$$\begin{aligned} \frac{dM_p}{dt} &= \nabla \cdot \langle (D_{\parallel} \mathbf{m}\mathbf{m} + D_{\perp} (I - \mathbf{m}\mathbf{m})) \cdot \nabla \mu \mathbf{m}\mathbf{m} \rangle \\ &= (D_{\parallel} - D_{\perp}) \left[\nabla \nabla : Q + U_0 \nabla \cdot (\nabla v * g_{\varepsilon} \cdot Q - \nabla M * g_{\varepsilon} : P) \right] \\ &\quad + D_{\perp} \left[\Delta M + U_0 \nabla \cdot (\nabla v * g_{\varepsilon} M - \nabla M * g_{\varepsilon} : Q) \right], \end{aligned} \quad (3.1b)$$

$$\begin{aligned} \frac{dM_r}{dt} &= -\bar{D}_r \langle \mathcal{R} \mu \cdot \mathcal{R}(\mathbf{m}\mathbf{m}) \rangle \\ &= -2\bar{D}_r \left[(3M - \nu I) - U_0 (M * g_{\varepsilon} \cdot M + M \cdot M * g_{\varepsilon} - 2M * g_{\varepsilon} : Q) \right], \end{aligned} \quad (3.1c)$$

$$\frac{dM_u}{dt} = \langle (\mathbf{m} \times \kappa \cdot \mathbf{m}) \cdot \mathcal{R}(\mathbf{m}\mathbf{m}) \rangle = \kappa \cdot M + M \cdot \kappa^T - 2\kappa : Q. \quad (3.1d)$$

Meanwhile, the stress and body force are expressed by moments as

$$\mathbf{F}^e = -\nabla g_{\varepsilon} * (\nu I - M) : M, \quad (3.2a)$$

$$\tau^p = \zeta_r D : Q = \zeta_r \kappa : Q, \quad (3.2b)$$

$$\tau^e = (3M - \nu I) - U_0 (M \cdot M * g_{\varepsilon} + M * g_{\varepsilon} \cdot M - 2M * g_{\varepsilon} : Q). \quad (3.2c)$$

3.1 Bingham closure approximation

The system (3.1) is not closed, because the second-order moment equation includes higher order moments Q and P , which are also unknown. We must evaluate Q and P using the value of M to close it. There are various ways to express Q and P as a function of M , including quadrature closure, Hinch and Leal closures, and the Bingham closure. Because M does not provide enough information to determine Q and P , any expression of Q and P is rigorous only in special cases. For example, the quadrature closure approximation is rigorous in perfect nematic phase. Feng et al. [7] examined the performance of five commonly used closures by numerical simulations and found that the Bingham closure was better than others.

In the process of Bingham closure approximation, the following function called as Bingham distribution, is taken as the reference CDF f to evaluate Q and P

$$f_b(\mathbf{m}) = \frac{1}{z} \exp(\mathbf{m} \cdot B \cdot \mathbf{m}), \quad (3.3)$$

where B is a symmetric second-order tensor and z is the normalization constant. If M is given, then there is one and only one B determined by

$$M = \int_{|\mathbf{m}|=1} \frac{1}{z} \exp(\mathbf{m} \cdot B \cdot \mathbf{m}) \mathbf{m} \mathbf{m} d\mathbf{m}. \quad (3.4)$$

So, each M determines one unique Bingham distribution, denoted by f_M . The fourth-order moments Q and sixth-order moments P are then evaluated by

$$Q = \langle \mathbf{m}^4 \rangle_{f_M}, \quad (3.5)$$

and

$$P = \langle \mathbf{m}^6 \rangle_{f_M}. \quad (3.6)$$

It is easy to check that the distribution f_M is the solution of the constrained optimization problem

$$- \int \psi \ln \psi d\mathbf{m} \rightarrow \max, \quad \langle \mathbf{m} \mathbf{m} \rangle_\psi = M, \quad (3.7)$$

where $\langle (\cdot) \rangle_\psi = \int (\cdot) \psi d\mathbf{m}$. Similar reference distributions could be obtained by solving

$$- \int \psi \ln \psi d\mathbf{m} \rightarrow \max, \quad \langle \mathbf{m}^i \rangle_\psi = M_i, \quad i = 2, 4, 6, \dots \quad (3.8)$$

This approach for obtaining reference distributions is called the maximum entropy principle [28] or the quasi-equilibrium approximation [14, 20, 21].

However, the functions $Q(M)$ and $P(M)$ determined by Eqs. (3.4)-(3.6) are all in implicit forms. Ilg et al. [20] proposed an evolution equation of B by Legendre transformation which avoids calculating Q and P from M by Newton's method at every time

step. However, it still cannot avoid evaluating M , Q and P from B by numerical integrations at every time step. So the computational cost is almost as expensive as Newton's method. On the other hand, the functions $Q(M)$ and $P(M)$ can be well approximated by polynomials or tensor polynomials. Chaubal and Leal [1] transformed Q into a diagonal coordinate system and represented its nonzero components as polynomials of the eigenvalues of M with coefficients determined by the least-square method. Grosso et al. [15] presented an approximated explicit form of $Q(M)$, which is an application of the invariant-based fitting method.

3.2 Energy dissipation

The QEA for general dissipative systems is discussed in length by Gorban et al. [11, 13]. One of the most important properties of the QEA is that it maintains the energy dissipation of the kinetic model.

Here in our model reduction, there is some difference to the systems studied in [11, 13]. We use local QEA to reduce the full kinetic model with nonlocal potential. However, the energy dissipation is still guaranteed. Now we prove that the energy dissipation of this reduced system is consistent with the exact kinetic system.

The free energy of the reduced system is defined as

$$A[M] = A[f_M] = \int_{\Omega} (B - \ln z I) : M - \nu + \frac{U_0}{2} g_{\varepsilon^*}(\nu I - M) : M \, d\mathbf{x}, \quad (3.9)$$

and the chemical potential μ at the reference distribution f_M is

$$\mu_{f_M} = \bar{\mu}_M : \mathbf{m}\mathbf{m}, \quad (3.10)$$

where

$$\bar{\mu}_M = (B - \ln z I) + U_0 g_{\varepsilon^*}(\nu I - M).$$

Taking the time derivative in both sides of (3.4), we get

$$\frac{dM}{dt} = \frac{d}{dt} (B - \ln z I) : Q, \quad (3.11)$$

and

$$\frac{d\nu}{dt} = \frac{d}{dt} (B - \ln z I) : M. \quad (3.12)$$

If we denote $\bar{U} = U_0 g_{\varepsilon^*}(\nu I - M)$, then the time derivative of free energy reads

$$\frac{dA[M]}{dt} = \int_{\Omega} \bar{\mu}_M : \frac{dM}{dt} + \frac{1}{2} \left(\frac{d\bar{U}}{dt} : M - \bar{U} : \frac{dM}{dt} \right) d\mathbf{x}.$$

Energy dissipation in the isolated isothermal system is

$$\begin{aligned}
T \frac{dS}{dt} &= -\frac{d}{dt} \left(\int_{\Omega} \frac{1}{2} \rho \mathbf{u} \cdot \mathbf{u} dx + A[M] \right) \\
&= -\int_{\Omega} \mathbf{u} \cdot \rho \frac{d\mathbf{u}}{dt} dx - \int_{\Omega} \bar{\mu}_{f_M} : \frac{dM}{dt} dx - \frac{1}{2} \int_{\Omega} \frac{d\bar{U}}{dt} : M - \bar{U} : \frac{dM}{dt} dx \\
&= \int_{\Omega} \eta_s \nabla \mathbf{u} : \nabla \mathbf{u} + \xi_r \kappa : Q : \kappa dx + \int_{\Omega} \left[\tau^e : \nabla \mathbf{u} - \bar{\mu}_M : \frac{dM}{dt} \right] dx \\
&\quad - \int_{\Omega} \left[\mathbf{F}^e \cdot \mathbf{u} + \frac{1}{2} \left(\frac{d\bar{U}}{dt} : M - \bar{U} : \frac{dM}{dt} \right) \right] dx. \tag{3.13}
\end{aligned}$$

Here the hydrodynamic equation (2.9) is used in the last step. The first term on the right hand side of (3.13) is non-negative provided that the coefficient η_s is non-negative. The third term is zero; the derivation of which is exactly the same as the microscopic case (see [31] for detail). For the second term, substituting Eq. (3.1) into the second term of (3.13), we get

$$\begin{aligned}
&\int_{\Omega} \left[\tau^e : \nabla \mathbf{u} - \bar{\mu}_M : \frac{dM}{dt} \right] dx \\
&= \int_{\Omega} \left[\tau^e : \nabla \mathbf{u} - \bar{\mu}_M : \frac{dM_u}{dt} dx - \int_{\Omega} \bar{\mu}_M : \frac{dM_p}{dt} + \bar{\mu}_M : \frac{dM_r}{dt} dx \right. \\
&= \int_{\Omega} \left[\tau^e : \nabla \mathbf{u} - \bar{\mu}_M : \langle (\mathbf{m} \times \kappa \cdot \mathbf{m}) \cdot \mathcal{R}(\mathbf{m}\mathbf{m}) \rangle_{f_M} \right] dx \\
&\quad - \int_{\Omega} \bar{\mu}_M : \nabla \cdot \langle (D_{\parallel} \mathbf{m}\mathbf{m} + D_{\perp} (I - \mathbf{m}\mathbf{m})) \cdot \nabla \mu_{f_M} \mathbf{m}\mathbf{m} \rangle_{f_M} dx \\
&\quad - \int_{\Omega} \bar{\mu}_M : -\bar{D}_r \langle \mathcal{R} \mu_{f_M} \cdot \mathcal{R}(\mathbf{m}\mathbf{m}) \rangle_{f_M} dx \\
&= \int_{\Omega} \left[\tau^e : \nabla \mathbf{u} - \langle (\mathbf{m} \times \kappa \cdot \mathbf{m}) \cdot \mathcal{R}(\bar{\mu}_M : \mathbf{m}\mathbf{m}) \rangle_{f_M} \right] dx \\
&\quad + \int_{\Omega} (\nabla \bar{\mu}_M)^T : \langle (D_{\parallel} \mathbf{m}\mathbf{m} + D_{\perp} (I - \mathbf{m}\mathbf{m})) \cdot \nabla \mu_{f_M} \mathbf{m}\mathbf{m} \rangle_{f_M} dx \\
&\quad + \bar{D}_r \int_{\Omega} \langle \mathcal{R} \mu_{f_M} \cdot \mathcal{R}(\bar{\mu}_M : \mathbf{m}\mathbf{m}) \rangle_{f_M} dx \\
&= \int_{\Omega} \langle \nabla \mu_{f_M} \cdot (D_{\parallel} \mathbf{m}\mathbf{m} + D_{\perp} (I - \mathbf{m}\mathbf{m})) \cdot \nabla \mu_{f_M} \rangle_{f_M} dx \\
&\quad + \bar{D}_r \int_{\Omega} \langle \mathcal{R} \mu_{f_M} \cdot \mathcal{R} \mu_{f_M} \rangle_{f_M} dx.
\end{aligned}$$

So the total energy dissipation

$$\begin{aligned}
T \frac{dS}{dt} &= \int_{\Omega} \eta_s \nabla \mathbf{u} : \nabla \mathbf{u} + \xi_r \kappa : Q : \kappa dx + \bar{D}_r \int_{\Omega} \langle \mathcal{R} \mu_{f_M} \cdot \mathcal{R} \mu_{f_M} \rangle_{f_M} dx \\
&\quad + \int_{\Omega} \langle \nabla \mu_{f_M} \cdot (D_{\parallel} \mathbf{m}\mathbf{m} + D_{\perp} (I - \mathbf{m}\mathbf{m})) \cdot \nabla \mu_{f_M} \rangle_{f_M} dx
\end{aligned}$$

is non-negative provided that η_s , ξ_r , \bar{D}_r , D_{\perp} and D_{\parallel} are all non-negative.

4 Numerical simulations

Several researchers have demonstrated that the Bingham closure quantitatively maintain the director dynamics of the Doi's theory in homogeneous flow except the flow-aligning attractor at high nematic potential. Feng et al. [7] compared the in-plane director dynamics of the Doi model and its Bingham closure model. Grosso et al. [15] analyzed the out-of-plane director dynamics. While these works focused on director dynamics in homogeneous flow, we are interested in defect dynamics and microstructure that cannot be described by the homogeneous Doi model.

In our simulation presented here, we restrict the distribution function in the shear plane, and assume that it is only nonhomogeneous in shear direction, i.e.,

$$f(\mathbf{x}, \mathbf{m}) = f(y, \cos\theta, \sin\theta), \quad \theta \in [0, 2\pi).$$

We take the macro velocity V_0 , the length of the macro domain L_0 , and the ratio L_0/V_0 as the units of velocity, length and time, respectively. Based on this choice of scales, the CDF is scaled by average number density of the LCP molecules \bar{v} . Then the dimensionless kinetic equations for LCP solutions in plane shear flow with isotropic long-range elasticity are given by

$$\begin{aligned} f_t &= \frac{\varepsilon^2}{De} \partial_y [((D_{\parallel}^* - D_{\perp}^*) \sin^2\theta + D_{\perp}^*) (f_y + fU_y)] + \frac{1}{De} \partial_{\theta} (f_{\theta} + fU_{\theta}) + u_y \partial_{\theta} (\sin^2\theta f), \\ u_t &= \frac{1-\gamma}{Re} u_{yy} + \frac{\gamma}{ReDe} \partial_y \tau_{12} - C, \\ \tau_{12} &= 2\langle \sin\theta \cos\theta \rangle - \langle U_{\theta} \sin^2\theta \rangle + \frac{De}{2} u_y \langle \sin^2\theta \cos^2\theta \rangle, \\ U &= \frac{U_0}{2} (\langle 1 \rangle * g_{\varepsilon} - \cos 2\theta \langle \cos 2\theta \rangle * g_{\varepsilon} - \sin 2\theta \langle \sin 2\theta \rangle * g_{\varepsilon}), \end{aligned}$$

where $De = \frac{V_0/L_0}{D_{r0}}$ is the Deborah number, $\varepsilon = l/L_0$ is the molecular length scaled by characteristic size of flow, Re is the Reynolds number and γ is the ratio of viscosity introduced by LCPs to the total viscosity of the solution,

$$Re = \rho \frac{V_0 L_0}{\eta_s + \nu \tilde{\zeta}_r}, \quad \gamma = \frac{\nu \tilde{\zeta}_r}{\eta_s + \nu \tilde{\zeta}_r}.$$

Moreover, $D_{\parallel}^*, D_{\perp}^*$ are nondimensional translational diffusion coefficients, C is the driven pressure gradient. We assume that the flow is homogeneous in x -direction and nonhomogeneous in y -direction (the shear direction).

The corresponding second-order moment model is obtained by letting

$$\mathbf{F}^e = 0, \quad \kappa = \begin{pmatrix} 0 & u_y \\ 0 & 0 \end{pmatrix}$$

in Eqs. (3.1)-(3.2) where M is a 2×2 matrix.

For the full kinetic model, a second-order finite difference scheme was used in y and θ direction. For the reduced moment model, similar second-order finite difference scheme was used for spatial discretization. A fourth-order Runge-Kutta scheme was used for time-stepping for both kinetic and reduced model. In the reduced model, the Bingham closure is implemented by the invariant-based fitting method.

According to the Cayley-Hamilton theorem, fourth-order moments Q as a function of M has following form

$$Q_{ijkl} = \nu\beta_1\mathcal{S}(\delta_{ij}\delta_{kl}) + \beta_2\mathcal{S}(\delta_{ij}M_{kl}) + \beta_3\mathcal{S}(M_{ij}M_{kl})/\nu, \tag{4.1}$$

where \mathcal{S} is the symmetric operator

$$\mathcal{S}(X_{i_1i_2\dots i_n}) = \frac{1}{n!} (X_{i_1i_2\dots i_n} + X_{i_2i_1\dots i_n} + \dots).$$

Parameters $\beta_1, \beta_2, \beta_3$ depend only on the invariants of M . Since the constrains $Q_{ijkk} = M_{ij}$ leads to two equations of $\beta_i, i = 1, 2, 3$, so only one parameter needs to be determined. We express this parameter as polynomial of invariants of M and fit the coefficients of the polynomial by using least-square method on (3.4) and (3.5). The results are given below:

$$\begin{aligned} \beta_2 &= 1 - \beta_3, \\ \beta_1 &= \left(\frac{\Pi}{2} + \frac{1}{8}\right)\beta_3 - \frac{1}{8}, \\ \beta_3 &= -69.8537\Pi^4 + 12.9169\Pi^3 + 10.8627\Pi^2 - 4.4474\Pi + 1.0023, \end{aligned}$$

where $\Pi = \det(M/\nu)$. The fitting error of Q is lower than 5×10^{-4} . Similar techniques were used to calculate the sixth-order moments P_{22ijkl} in the translational diffusion term. The details are included in the appendix.

The bifurcation diagram for homogeneous flow (Fig. 1) shows that the Bingham closure model fails to predict flow-aligning when both the nematic potential and the Deborah number are high. The position of the homoclinic bifurcation line predicted by the reduced model ($U_0 < 5.10$) is slightly different from that predicted by the exact kinetic model ($U_0 < 4.88$). This means that the error introduced by the Bingham closure decays slower than the perturbation introduced by shear when the Deborah number goes to zero. Except that, the Bingham model agrees with the exact kinetic model well for the moderate U_0 , especially in the region $(U_0, De) \in [5.2, 6.5] \times [0, 5]$. Indeed, this region is the most interesting part of the parameter region, which can produce rich dynamic pattern in nonhomogeneous system.

For nonhomogeneous flow, we study the Couette flow and the Poiseuille flow.

In the simulation, we fix $\varepsilon = 0.02, D_{\perp}^* = 0, D_{\parallel}^* = 0.2, Re = 1$, and vary U_0 and De . The molecules on the two boundaries are anchored along the flow direction. Similarly, the reduced model by the Bingham closure agrees with the exact kinetic model qualitatively, except in the high Deborah number region. For any fixed $U_0 > 5.0$ in Couette flow, when

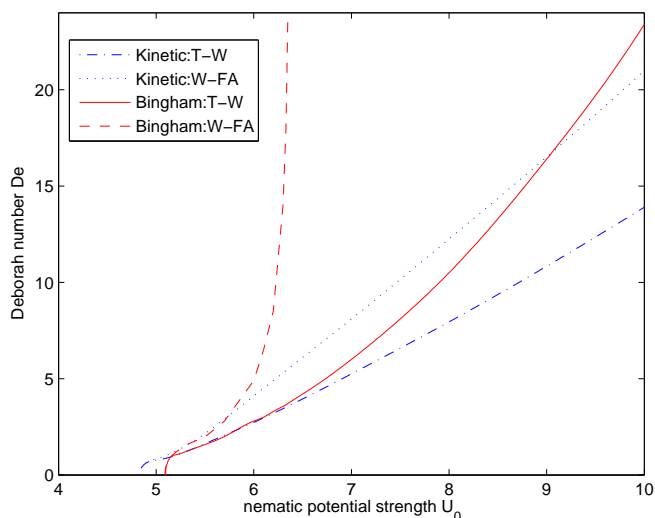


Figure 1: The bifurcation diagram of the Bingham closure model and the kinetic model in homogeneous flow. The dotted line is the wagging and flow-aligning bifurcation line of the kinetic model. The dash-dot line is the tumbling and wagging bifurcation line of the kinetic model. The dashed line is the wagging and flow-aligning bifurcation line of the Bingham model. The solid line is the tumbling-wagging bifurcation line of the Bingham model.

the Deborah number increases from zero to a very high value, the exact kinetic model predicts five dynamic modes of director configuration [32] (a different potential was used in [32], but similar dynamic modes are predicted): a) ES: elastic-driven steady state; b) T: tumbling state; c) TWD: tumbling-wagging composite state with inside defects; d) W: wagging state; e) VS: viscous-driven steady state. For moderate U_0 , the reduced model predicts all these five modes (Fig. 2).

The reduced model does not quantitatively agree with the exact kinetic model (Figs. 3 and 4). The two main differences in tumbling periods and defect positions results from Bingham closure's failure to describe the skewed distribution function. The tumbling rate predicted by the Bingham closure model is slower; the defect positions are different (Fig. 3). Fig. 5 shows the errors between the true CDF and the corresponding reference Bingham distribution in an exact kinetic simulation. It is observed that errors near the boundaries are much larger than those in the inner bulk region, and the maximum is reached near the boundary defects because boundary anchoring skews the distribution function.

5 Conclusion and comments

We have proposed a general kinetic-hydrodynamic coupled model with translational diffusion and an integral nonlocal intermolecular potential. The integral potential concerned in this model can derive the well-known Marrucci-Greco potential in some special

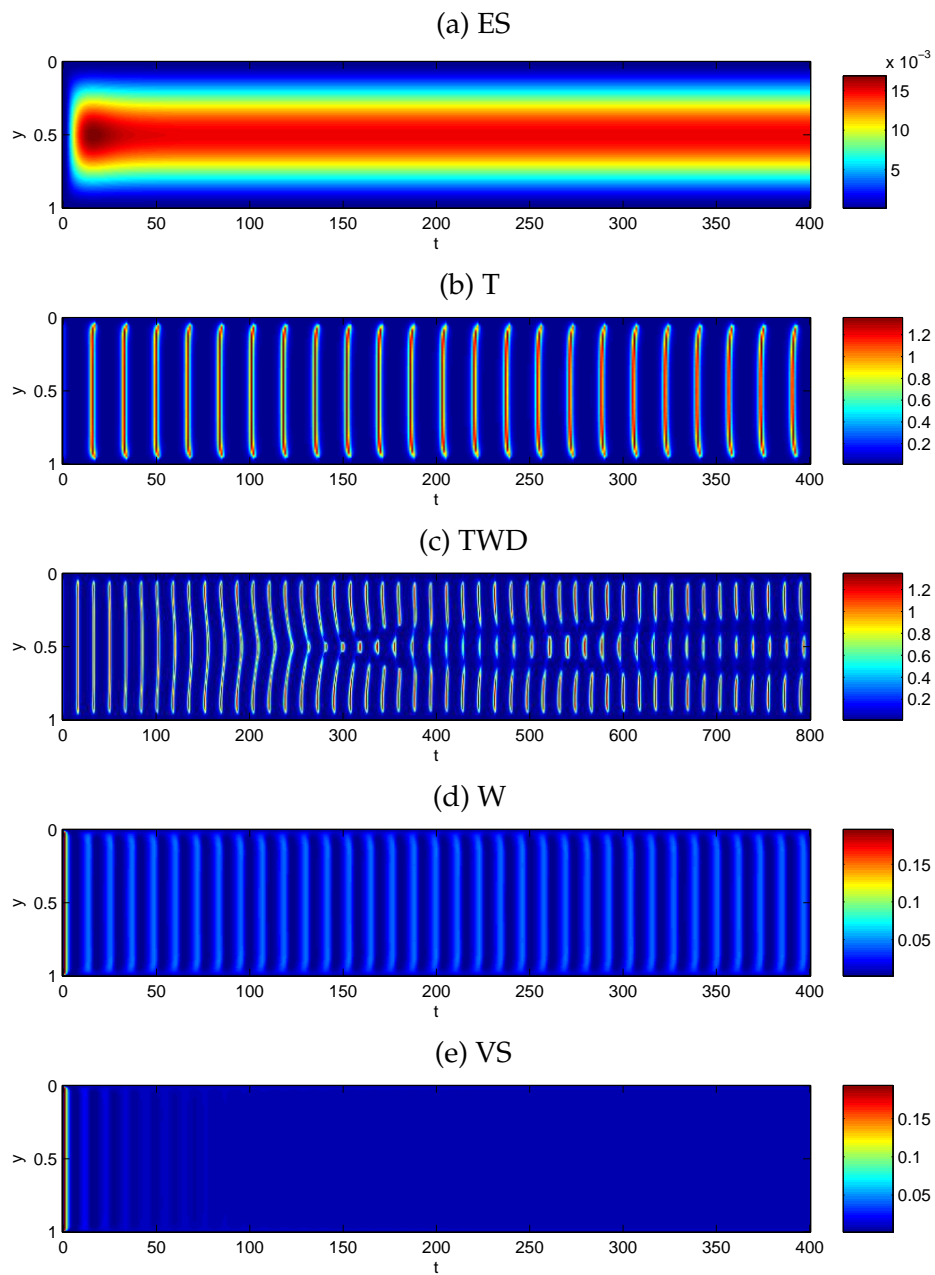


Figure 2: The director configurations of five modes in Couette flow predicted by Bingham closure model at $U_0=6.0$. (a) ES: elastic-driven steady state, $De=0.01$; (b) T: tumbling state, $De=1.0$; (c) TWD: tumbling-wagging composite state with inside defects, $De=2.0$; (d) W: wagging state, $De=4.0$; (e) VS: viscous-driven steady state, $De=6.0$. Colors represent the director angle. The horizontal axis is dimensionless time and the vertical axis is the distance to lower slab.

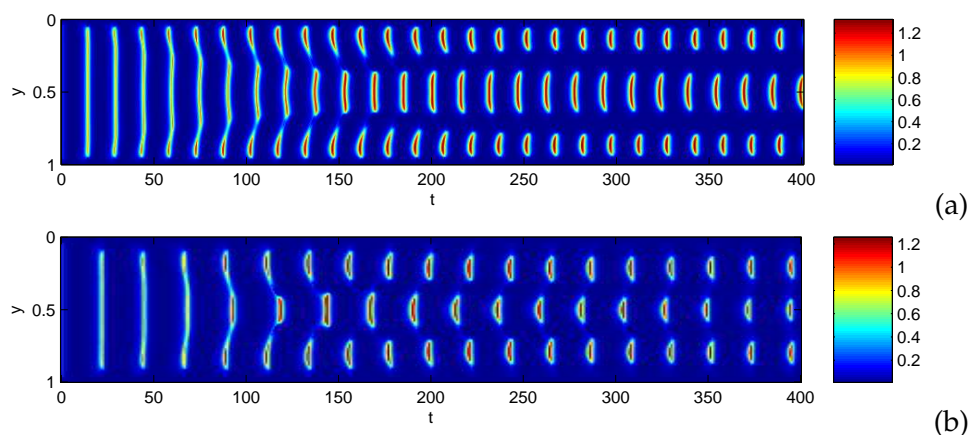


Figure 3: The typical TWD modes in Couette flow at $U_0 = 5.5$, $De = 1.5$. (a) the exact kinetic model, (b) the Bingham closure model. Colors represent the director angle. The horizontal axis is dimensionless time and the vertical axis is the distance to lower slab.

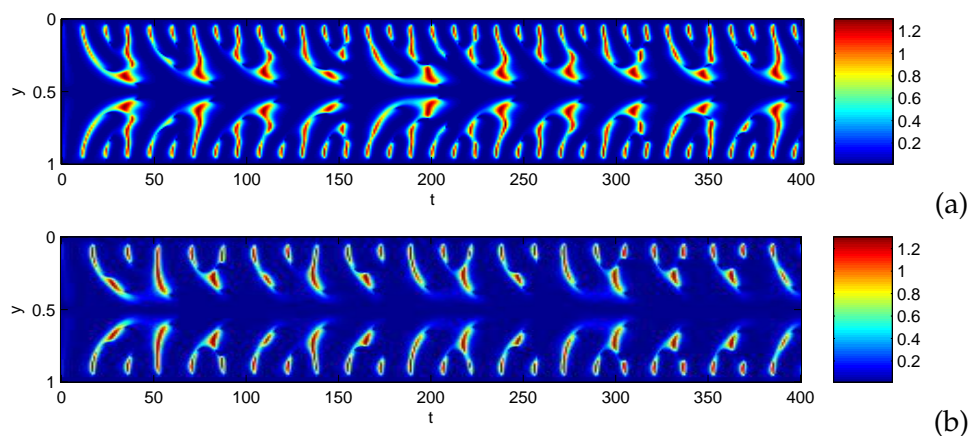


Figure 4: The typical orientational configuration in Poiseuille flow. $U_0 = 5.5$, $De = 1.0$. (a) the exact kinetic model, (b) the Bingham closure model. Colors represent the director angle. The horizontal axis is dimensionless time and the vertical axis is the distance to lower slab.

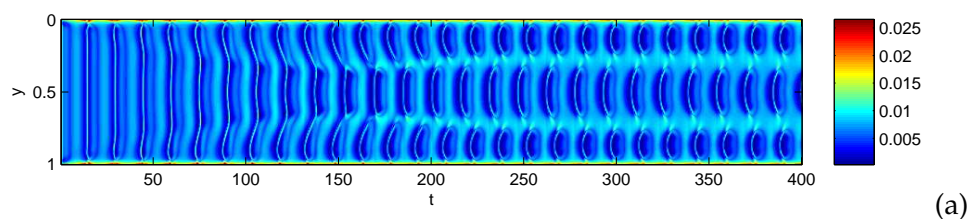


Figure 5: The error of the Bingham closure in every time step of exact kinetic simulation. $U_0 = 5.5$, $De = 1.5$. The horizontal axis is dimensionless time and the vertical axis is the distance to lower slab.

cases. We deduced a moment model by using the quasi-equilibrium closure approximation, which happens to be Bingham closure in second-order moment case. We also proved that the energy dissipation is maintained for the reduced moment model.

In the numerical simulation, the invariant-based fitting method is implemented. Numerical results of the in-plane rotational case show that the second-order moment model can qualitatively predict the dynamics of defects and microstructure when the nematic potential strength is not very high. But when the nematic potential strength is high, the second-order model fails to predict flow-aligning at high shear rate, due to the Bingham closure's failure to describe skewed distribution functions. Our nonhomogeneous simulations also show that the CDF is always skewed near the boundary defects. The numerical results also show that the translational diffusion term, which is often discarded plays an important role in defect dynamics, e.g., the generation of TWD mode.

The kinetic model for the LCP solutions is such a complex nonlinear system. So far, no second-order moment model was reported that can predict quantitatively the bifurcation phase diagram of the full kinetic model. To be more accurate, one needs to put more moments in the reduced model. This is actually a trade off between accuracy and numerical effort.

Nevertheless, the second-order moment model is the simplest one for systems with isotropic long-range elasticity; for systems with anisotropic long-range elasticity, the fourth-order moment model is needed to guarantee energy dissipation if one uses the natural QEA closure. Implementing such a model by the invariant-based fitting method involves fitting higher moments up to tenth-order. Although it is very complicated, one can extend invariant-based fitting method to higher-order tensors approximation [23] to build a relatively accurate higher-order moment model.

Acknowledgments

The authors would like to thank Prof. Sharon Murrel for her help in revising English. The research of Pingwen Zhang is partially supported by the State Key Basic Research Project of China 2005CB321704 and the National Science Foundation of China for Distinguished Young Scholars 10225103. The research of Guanghua Ji is partially supported by National Science Foundation of China 10801014.

Appendix

Here we describe how to estimate sixth-order moment tensor P in terms of second-order moment tensor M by invariant-based fitting method for the Bingham closure. For simplicity, we assume $\nu = 1$. By the Cayley-Hamilton theorem, we can write P as

$$P_{ijklmn} = \beta_1 \mathcal{S}(\delta_{ij}\delta_{kl}\delta_{mn}) + \beta_2 \mathcal{S}(M_{ij}\delta_{ij}\delta_{mn}) + \beta_3 \mathcal{S}(M_{ij}M_{kl}\delta_{mn}) + \beta_4 \mathcal{S}(M_{ij}M_{kl}M_{mn}),$$

where β_i , $i = 1, 2, 3, 4$ are functions of the invariants of M , i.e., $\Pi = \det(M)$, as the first invariant of M is 1. The constraint $P_{ijkknm} = M_{ij}$ leads to the following relationships of $\beta_i, i = 1, 2, 3, 4$

$$\begin{aligned}\beta_2 &= \frac{15}{16} - \beta_3 - \frac{1}{16}(15 - 12\Pi)\beta_4, \\ \beta_1 &= -\frac{5}{32} + \left(\frac{1}{8} + \frac{1}{9}\Pi\right)\beta_3 + \left(\frac{5}{32} - \frac{3}{8}\Pi\right)\beta_4.\end{aligned}$$

Then we assume β_3, β_4 are polynomials of Π

$$\beta_3 = \sum_{i=0}^n c_i \Pi^i, \quad \beta_4 = \sum_{i=0}^n c'_i \Pi^i.$$

To estimate the coefficients c_i, c'_i , $i = 1, \dots, n$, we take N samples of Bingham distributions, and the corresponding values of $M_{11}, P_{111111}, P_{111122}$ are obtained by direct numerical integration. Then we determine the values of the coefficients c_i, c'_i , $i = 1, \dots, n$ by the least-square method. In our procedure, we take $n = 2, N = 600$. The polynomials of β_3, β_4 are then given by

$$\begin{aligned}\beta_3 &= -64.334\Pi^2 + 61.570\Pi - 0.1082, \\ \beta_4 &= 36.362\Pi^2 - 36.694\Pi + 1.0601.\end{aligned}$$

References

- [1] C. V. Chaubal and L. G. Leal. A closure approximation for liquid-crystalline polymer models based on parametric density estimation. *Journal of Rheology*, 42(1):177–201, 1998.
- [2] D. H. Chung and T. H. Kwon. Invariant-based optimal fitting closure approximation for the numerical prediction of flow-induced fiber orientation. *Journal of rheology*, 46(1):169–194, 2002.
- [3] J. S. Cintra, Jr. and C. L. Tucker III. Orthotropic closure approximations for flow-induced fiber orientation. *Journal of Rheology*, 39(6):1095, 1995.
- [4] M. Doi. Molecular dynamics and rheological properties of concentrated solutions of rodlike polymers in isotropic and liquid crystalline phases. *Journal of Polymer Science: Polymer Physics Edition*, 19:229–243, 1981.
- [5] M. Doi and S. Edwards. *The Theory of Polymer Dynamics*. Oxford University Press, Oxford, 1986.
- [6] W. E and P. Zhang. Ericksen-Leslie equation derived from a molecular kinetic equation under small Deborah number. *Methods and applications of analysis*, 13(2):181–198, 2006.
- [7] J. Feng, C. V. Chaubal, and L. G. Leal. Closure approximations for the Doi theory: Which to use in simulating complex flows of liquid-crystalline polymers? *Journal of Rheology*, 42(5):1095–1109, 1998.
- [8] J. J. Feng, G. Sgalari, and L. G. Leal. A theory for flowing nematic polymers with orientational distortion. *J. Rheol.*, 44(5):1085–1101, 2000.
- [9] M. G. Forest, Q. Wang, and R. Zhou. The flow-phase diagram of Doi-Hess theory for sheared nematic polymers II: finite shear rates. *Rheologica Acta*, 2004.

- [10] M. G. Forest, Q. Wang, and R. Zhou. The weak shear kinetic phase diagram for nematic polymers. *Rheologica acta*, 43:17–37, 2004.
- [11] A. Gorban, I. Karlin, and A. Zinovyev. Constructive methods of invariant manifolds for kinetic problems. *Physics Reports*, 396:197–403, 2004.
- [12] A. N. Gorban, P. A. Gorban, and I. V. Karlin. Legendre integrators, post-processing and quasiequilibrium. *J. Non-Newtonian Fluid Mech.*, 120:149–167, 2004.
- [13] A. N. Gorban and I. V. Karlin. *Invariant Manifolds for Physical and Chemical Kinetics*. Berlin-Heidelberg-New York: Springer, 2005.
- [14] A. N. Gorban, I. V. Karlin, P. Ilg, and H. C. Öttinger. Corrections and enhancements of quasi-equilibrium states. *Journal of Non-Newtonian Fluid Mechanics*, 96:203–219, 2001.
- [15] M. Grosso, P. L. Maffettone, and F. Dupret. A closure approximation for nematic liquid crystals based on the canonical distribution subspace theory. *Rheologica Acta*, 39:301–310, 2000.
- [16] S. Hess. Fokker-Planck-equation approach to flow alignment in liquid crystals. *Zeitschrift Naturforschung Teil A*, 31(A):1034–1037, 1976.
- [17] E. J. Hinch and L. G. Leal. Constitutive equations in suspension mechanics. Part II. Approximation forms for a suspension of rigid particles affected by Brownian rotations. *J. Fluid Mech.*, 76:187–208, 1976.
- [18] P. Ilg, I. Karlin, and H. Öttinger. Generating moment equations in the Doi model of liquid-crystalline polymers. *Phys. Rev. E*, 60(5):5783–5787, 1999.
- [19] P. Ilg, I. Karlin, and H. Öttinger. Reconstruction of constitutive equations from Brownian dynamics. In *Proceedings of the XIII International Congress on Rheology*, vol. 2, pp. 64–66, Cambridge, 2000.
- [20] P. Ilg, I. V. Karlin, M. Kröger, and H. C. Öttinger. Canonical distribution functions in polymer dynamics. (II). Liquid-crystalline polymers. *Physica A*, 319:134–150, 2003.
- [21] P. Ilg, I. V. Karlin, and H. C. Öttinger. Canonical distribution function in polymer dynamics. (I). Dilute solutions of flexible polymers. *Physica A*, 315:367–385, 2002.
- [22] D. A. Jack and D. E. Smith. An invariant based fitted closure of the sixth-order orientation tensor for modeling short-fiber suspensions. *Journal of Rheology*, 49(5):1091–1115, 2005.
- [23] D. A. Jack and D. E. Smith. Sixth-order fitted closures for short-fiber reinforced polymer composites. *Journal of Thermoplastic Composite Materials*, 19:217–246, 2006.
- [24] D. H. Klein, C. Garcia-Cervera, H. Ceniceros, and L. Leal. Computational studies of a model for nematic liquid crystalline polymers. In Rob May and A. J. Roberts, editors, *Proc. of 12th Computational Techniques and Applications Conference CTAC-2004*, 46:C210–C244, 2005.
- [25] D. H. Klein, C. Garcia-Cervera, H. Ceniceros, and L. Leal. Ericksen number and Deborah number cascade predictions of a model for liquid crystalline polymers for simple shear flow. *Physics of Fluids*, 19(2):023101, 2007.
- [26] R. G. Larson and H. Öttinger. Effect of molecular elasticity on out-of-plane orientations in shearing flows of liquid-crystalline polymers. *Macromolecules*, 24:6270–6282, 1991.
- [27] G. Marrucci and F. Greco. The elastic constants of Maier-Saupe rodlike molecule nematics. *Molecular crystals and liquid crystals*, 206:17–30, 1991.
- [28] M. van Gurp. Letter to the editor: On the use of spherical tensors and the maximum entropy method to obtain closure for anisotropic liquids. *J. Rheol.*, 42(5):1269–1271, 1998.
- [29] V. Verleye and F. Dupret. Numerical prediction of fiber orientation in complex injection molded parts. In *Proceedings of the ASME Winter Annual Meeting, MD*, volume 49. HTD-vol. 283, pp. 264–279, 1994.
- [30] Q. Wang. A hydrodynamic theory for solutions of nonhomogeneous nematic liquid crys-

- talline polymers of different configurations. *Journal of Chemical Physics*, 116:9120–9136, 2002.
- [31] Q. Wang, W. E, C. Liu, and P. Zhang. Kinetic theory for flows of nonhomogeneous rodlike liquid crystalline polymers with a nonlocal intermolecular potential. *Physical Review E*, 65, 2002.
- [32] H. Yu and P. Zhang. A kinetic-hydrodynamic simulation of microstructure of liquid crystal polymers in plane shear flow. *J. Non-Newtonian Fluid Mech.*, 141:116–127, 2007.